Quaternary Research **55**, 190–202 (2001)
doi:10.1006/qres.2001.2214, available online at http://www.idealibrary.com on IDEAL®

The Last Interglacial to Glacial Transition, Togiak Bay, Southwestern Alaska

Darrell S. Kaufman

Department of Geology and Department of Environmental Sciences, Northern Arizona University, Flagstaff, Arizona 86011-4099

E-mail: Darrell.Kaufman@nau.edu

William F. Manley and Alexander P. Wolfe

Institute of Arctic and Alpine Research, University of Colorado, Boulder, Colorado 80309-0450

Feng Sheng Hu

Department of Plant Biology, University of Illinois, 505 Goodwin Avenue, Urbana, Illinois 61801

Shari J. Preece and John A. Westgate

Physical Sciences Division, University of Toronto at Scarborough, Ontario MIC 1A4, Canada

and

Steve L. Forman

Department of Earth and Environmental Sciences, University of Illinois, Chicago, Illinois 60607-7059

Received August 9, 2000

An 18-m-high coastal bluff at Togiak Bay (northwestern Bristol Bay, southwestern Alaska) exposes marine, lacustrine, fluvial, glacial, volcanic, and organic deposits that record the ~50,000-year-long transition from the peak of the last interglaciation to the early Wisconsin glaciation. The base of the section is dominated by stratified sand and silt extending up to 4.3 m above sea level; marine diatoms are present, and pollen assemblages are characterized by relatively high percentages of *Picea, Alnus*, and *Betula* and low percentages of Poaceae and Cyperaceae. The marine sediment was probably deposited during the peak of marine oxygen-isotope stage (OIS) 5e. An infrared stimulated luminescence (IRSL) age of 151,000 ± 13,000 yr from near the base of the exposure is permissive of this correlation. The marine sand and silt are overlain by 0.8 m of peaty silt with diatoms that record a transition from marine to lacustrine conditions. During this interval, Poaceae and Cyperaceae dominate the pollen assemblages, and *Picea* and shrubs are nearly absent, suggesting that herb tundra occupied the landscape. This interval probably encompasses OIS 5d on the basis of the herb tundra and an IRSL age of 119,000 ± 10,000 yr from 60 cm below the marine/lacustrine transition. The organic mud is overlain by 3.1 m of stratified sand and organic silt that apparently record shallowing of the lake; reappearance of spruce and shrubs (=OIS 5c?); and subsequent deepening of the lake (=OIS 5b?); followed by aggradation of a floodplain (=OIS 5a?), which was dry at the time basaltic lava buried the site. Thermoluminescence analyses on lava-baked sediment indicate that the eruption occurred 70,000 ± 10,000 yr ago. Sometime thereafter, but prior to 53,600 ^{14}C yr B.P., an outlet of the Ahklun Mountains ice cap advanced over the site and deposited ~7 m of bouldery ice-contact drift. The sedimentary sequence contains at least four tephra beds. Major- and trace-element chemistry provide a basis for correlating two of the tephras with tephra beds at nearby sites. The tephras, luminescence ages, and correlations with marine isotope stages provide the geochronological control to place the Togiak Bay section into a global context. The site serves as an important new reference section for late Pleistocene paleoenvironmental change in eastern Beringia.

INTRODUCTION

Beringia is one of the few regions within the North American Arctic that mostly escaped late-Wisconsin glaciation and thus preserves an extensive geologic record of Quaternary paleoenvironmental changes. The coastal regions, where interstratified terrestrial and marine deposits are exposed, are particularly important. Sea-level changes recorded at these sites largely reflect the height of eustatic sea level modulated by the growth and decay of continental ice sheets and thereby provide a link to the global record of sea-level change. In a few places, superpositional stratigraphic relations between glacial deposits and marine sediments afford an opportunity to integrate the local record of glaciation with the global record of sea-level

0033-5894/01 $35.00

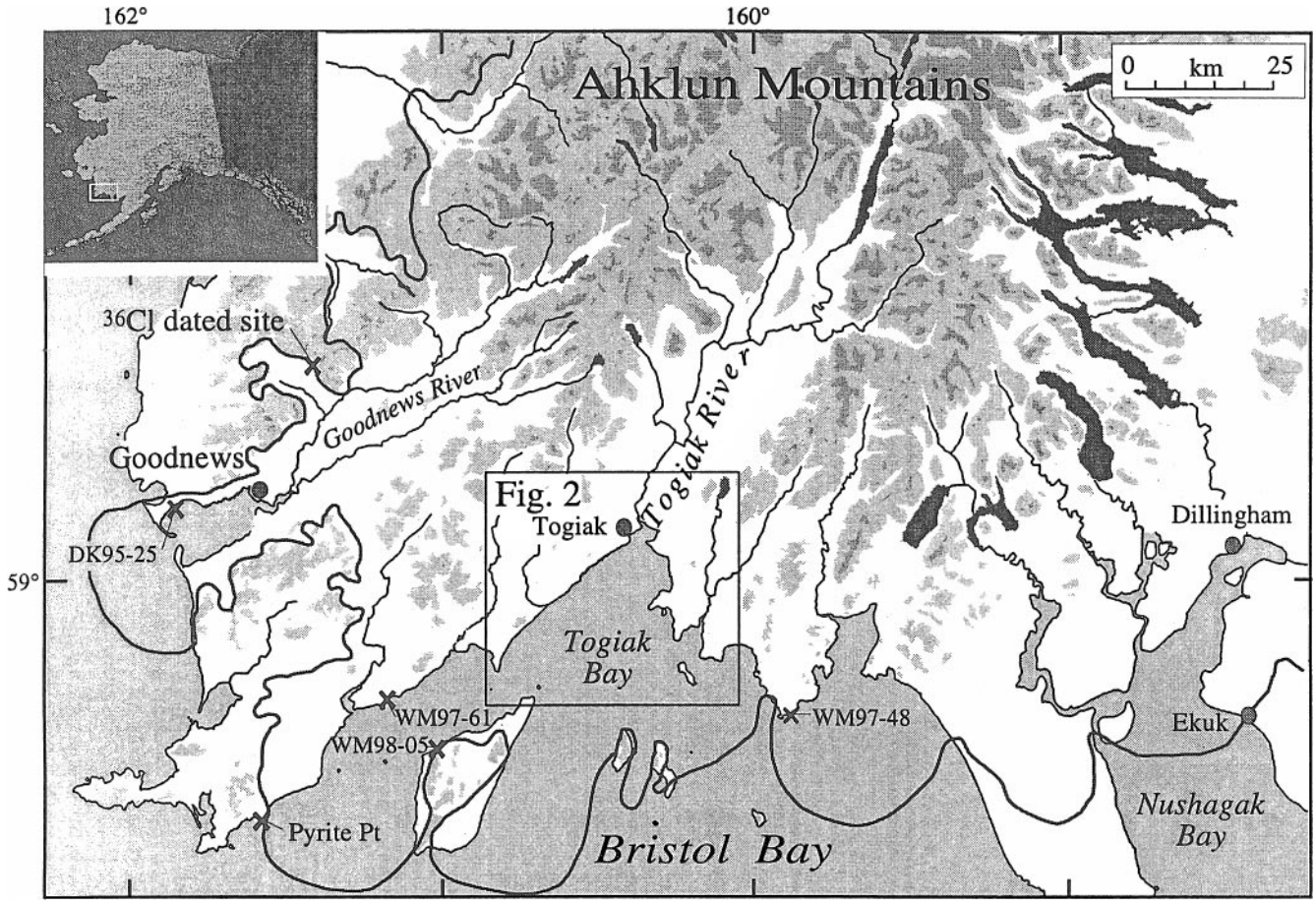

FIG. 1. The Northern Bristol Bay region, showing locations mentioned in text and the maximum extent of late Pleistocene glaciers. Ice-free areas within glacial limit are not shown. OCt, sites where Old Crow tephra was found. Light shading, >200 m elevation; darker shading, 600 m; darkest shading, modern lakes.

change (e.g., Hopkins, 1967). In southwestern Alaska, the Quaternary stratigraphic record is enhanced by the presence of interstratified volcanic materials. Widespread tephra beds provide a link to paleoenvironmental records from terrestrial and marine basins of Beringia (e.g., Carter *et al*., 1989; Péwé *et al*., 1997). Local basaltic lava flows, and other datable geological materials, provide the geochronological control needed to determine the timing of environmental changes interpreted from the geologic record.

This study focuses on a remarkable coastal exposure at Togiak Bay, southwestern Alaska, where two of us (DSK and WFM) discovered an 18-m-thick sequence of interstratified marine, lacustrine, fluvial, glacial, volcanic, and organic deposits. Geochronological, sedimentological, and paleoenvironmental data indicate that the sequence extends from the last interglaciation (marine oxygen-isotope substage 5e) to the early Wisconsin and records the transition to glacial conditions of the late Pleistocene. Such stratigraphic records provide insights into environmental changes that result from fluctuating climatic boundary conditions. The last interglacial period is particularly important because it offers an analog of environmental response to warmer-than-present temperatures. This study contributes to a growing database of paleoclimatic data for the last interglacial period in Alaska (e.g., Hamilton and Brigham-Grette, 1991; Brigham-Grette and Hopkins, 1995) and other areas of the Arctic (e.g., Matthews, 1991; Schweger and Matthews, 1991; Brigham-Grette *et al*., 2001).

The study site is located at Togiak Bay, on the northwestern edge of Bristol Bay in the eastern Bering Sea (Fig. 1). The Togiak River, the principal drainage into Togiak Bay, enters from the north. The river heads in the highest elevations of the Ahklun Mountains, flows south–southwest through a broad valley flanked by rugged massifs and rolling uplands, and then debouches onto the coastal lowlands. The valley is a graben formed in highly deformed rocks of Mesozoic age and bounded by northeast-trending faults comprising the southwestern extension of the Denali fault system (Hoare and Coonrad, 1978a). It was repeatedly glaciated during pre-late-Wisconsin advances when an outlet of the Ahklun Mountains ice cap extended beyond the present-day coast and spread onto the continental shelf (Kaufman *et al*., 2001; Manley *et al*., 2001). The limits of the glacier advances are marked by broad belts of hummocky drift and ice-thrust ridges that form the main topographic features in the lowlands around Togiak Bay. Coastal retreat has exposed

surficial deposits around the bay, bordered by bedrock headlands.

The Togiak Bay area presently experiences a subarctic maritime climate. Mean July temperature at nearby Dillingham is 13°C, and mean January temperature is −9°C (NCDC 1961–1990 normals, Western Regional Climate Center). The area is within the zone of discontinuous permafrost. Low-shrub tundra is the predominant vegetation community, with tussock tundra in low-lying areas (Gallant *et al.*, 1995). *Salix* (willow), *Betula nana* (dwarf arctic birch), *B. glandulosa* (resin birch), Ericaceae (e.g., *Arctostaphylos alpina, Vaccinium vitis-idaea, Empetrum nigrum*), and Cyperaceae (sedges) are dominant. Extensive shrub thickets of *Alnus crispa* (green alder) occupy mountain slopes and riparian zones. The range limit of *Picea* (spruce) is about 40 km to the east, where it extends into valleys that penetrate the eastern piedmont of the Ahklun Mountains.

LITHOSTRATIGRAPHY

The surficial deposits surrounding Togiak Bay were studied in numerous coastal bluffs. Here we focus on an 18-m-high exposure at the southeastern corner of Togiak Bay (58° 58.57′ N; 161° 20.87′ W; Fig. 2). A hand level and measuring tape were used to measure vertical heights relative to mean high tide. The lower 2.5 m of the outcrop is covered by colluvium. Above that, the exposure can be subdivided into three main sections: a lower sequence of stratified sand and silt, a basaltic lava flow, and an upper sequence of bouldery gravel.

The lower stratified sequence is dominated by very fine to medium grained sand interstratified with three zones of autochthonous peaty silt and four tephra beds (Fig. 3). The sediment is weakly deformed, with most beds laterally continuous over tens of meters. The lower stratified sequence can be subdivided into three lithofacies units.

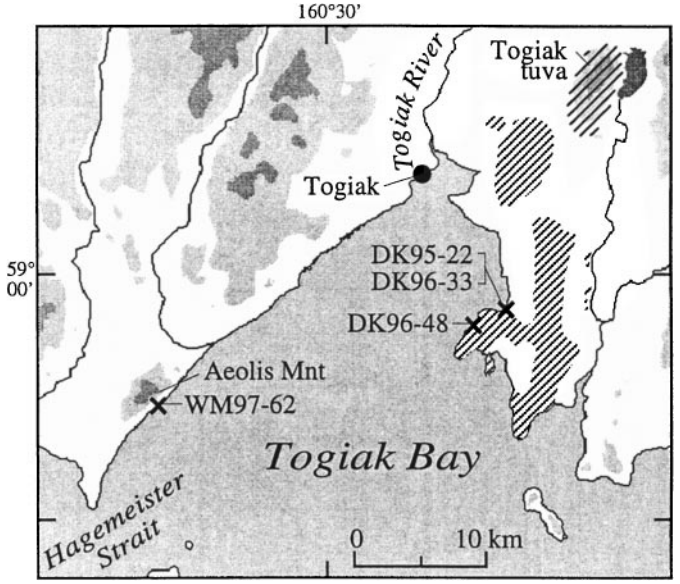

FIG. 2. Togiak Bay showing sample locations and geographic features mentioned in text. Diagonally hatched area is mapped as Pliocene–Pleistocene basalt by Hoare and Coonrad (1961a,b). Map location is shown in Fig. 1. Light shading, >100 m elevation; darker shading, >250 m; darkest shading, modern lake.

(1) The basal unit, from 2.5 to 3.6 m above sea level (asl), is composed of 1- to 3-cm-thick beds of tan, fine to very fine sandy silt, with abundant ripple and horizontal lamina. The lower half of the lithofacies unit contains three 5-cm-thick beds of ripple cross-laminated, oxidized, medium sand; the upper half contains many 1- to 2-cm-thick beds of massive, oxidized, medium sand.

(2) The second lithofacies unit, lying conformably over the sand, extends from 3.6 to 5.1 m asl and is dominated by blue–gray massive silt and clay. The lower 0.6 m of this unit (below 4.3 m asl) is inorganic and contains coarse sand and scattered stones (<2%) up to 2 cm in diameter. The upper 20 cm shows faint partings of sand along roughly horizontal bedding planes. The mud is interrupted at 3.8 m asl by a 20-cm-thick bed of gray, indurated, granule–pebble diamicton (subrounded clasts up to 5 cm in diameter comprise ∼40% of the bed) bounded by an undulating basal contact and a sharp upper contact. At 4.5 m asl and upward, the mud is dark, organic rich, and faintly bedded; in places, it contains 1-cm-thick beds of peaty mud with abundant macrofossils of fibrous vegetation.

(3) The upper lithofacies unit (unit 3, Fig. 3) extends from 5.1 to 8.3 m asl and is dominated by dark gray to olive gray, medium and fine grained sand. The lower 40 cm contains beds, 0.5 to 2.0 cm thick, of fibrous peaty sand separated by massive silty sand. Upward, the sand is generally coarser grain with medium sand separated by thin (<1 cm) silty sand interbeds. A chaotic zone, 3 to 5 cm thick, of angular intraclasts of peaty silt is found at 6.4 m asl. The unit contains two beds of massive to laminated, organic-rich mud: at 6.5 to 6.6 and at 7.4 to 7.8 m asl. The upper bed is much more silty than the lower one. It contains a few sandy interbeds in the lower 10 cm and grades upward into massive, indurated, reddish–brown silt. In addition, a 2-cm-thick bed of black, indurated mud caps the lithofacies unit and appears to have contained organics prior to being baked by the overlying lava. At 6.8 m asl, the sand is interrupted by a 5- to 20-cm-thick bed of iron-cemented, granule–pebble gravel. The unit also contains four tephra beds (see below).

The exposed stratified sand and mud between 2.6 and 8.3 m asl was sampled at 20-cm intervals (5-cm-thick samples; Fig. 3). For each sample, we measured mass magnetic susceptibility (MS) of the <2.0-mm fraction using a Bartington MS-2 meter, total organic carbon (TOC) using a coulometer, and particle size using a Malvern laser analyzer. The MS exhibits high values over the lower 1.6 m of the exposed section (Fig. 3). Between 4.2 and 4.4 m asl, MS decreases sharply from values of >10 to $<2 \times 10^{-7}$ m^3 kg^{-1}. MS values remain low upward in the section, except in the gravel at ∼7 m asl. The transition from high to low MS corresponds with the shift from inorganic to variably organic-rich mud in the second lithofacies unit. MS is generally related inversely to organic matter content. TOC is

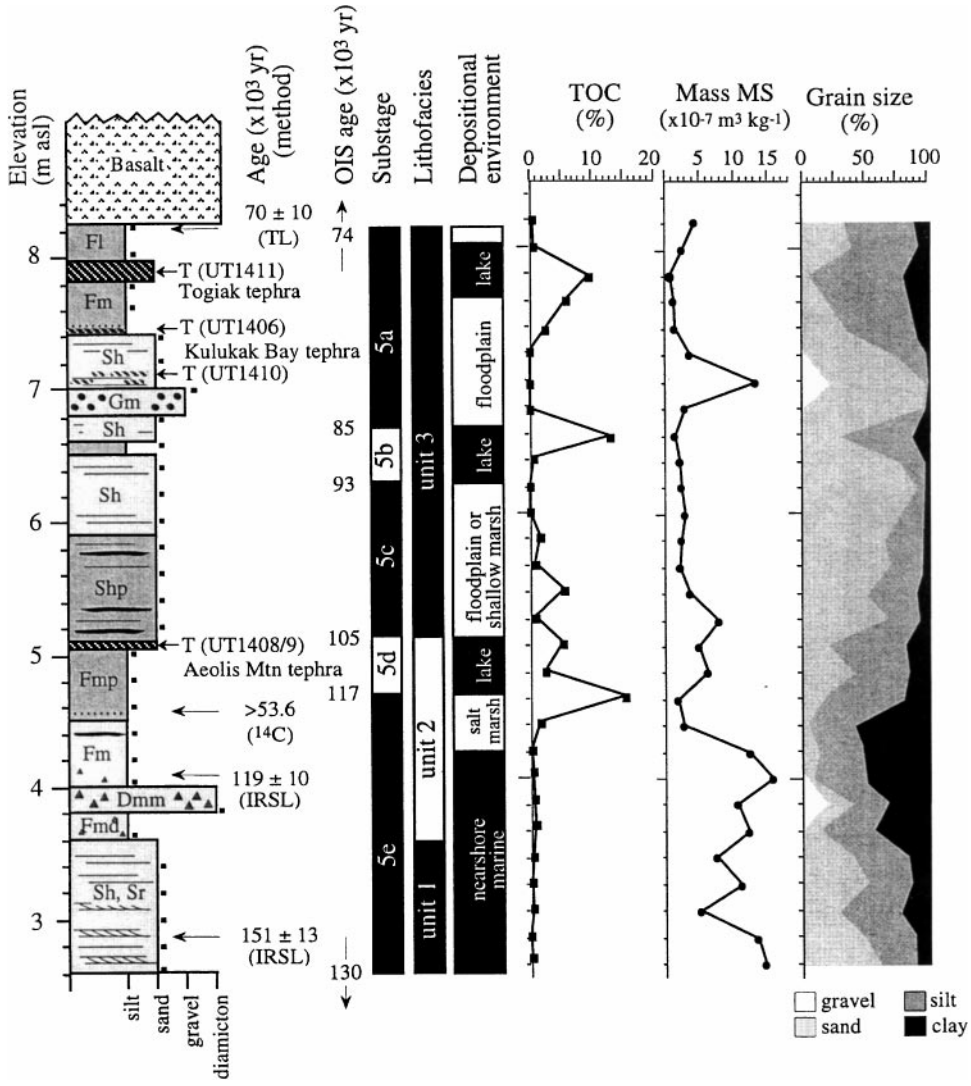

FIG. 3. Stratigraphy of the lower stratified sequence at the Togiak Bay site (DK96-33). Basalt is 3.1 m thick and is overlain by 6.8 m of silty boulder gravel (Ice-contact drift). Sampled levels are indicated by solid squares; T, tephra (diagonally hatched); lithofacies codes modified from Eyles and Miall 1984; p, peaty); OIS, correlated marine oxygen-isotope stage; OIS ages according to Martinson *et al*. (1987). Magnetic susceptibility (MS), grain size, and total organic carbon (TOC) content are also shown.

<1% below 4.5 m asl and then reaches values as high as 10–15% in three intervals between 4.5 and 8.0 m asl. The grain-size and MS data distinguish the three main lithofacies units.

The lower stratified sequence is overlain by a 3.1-m-thick flow of vesicular basalt. The lava flow was mapped previously in reconnaissance-scale studies by Hoare and Coonrad (1961a,b). It is one of several isolated Plio–Pleistocene lava flows in the lower Togiak River valley composed of finely porphyritic, olivine basalt. The source of the lava is not known. The single obvious volcano in the area, the Togiak Tuya (Fig. 2; Hoare and Coonrad, 1978b), is too old (Kaufman *et al*., 2001). If a cone was constructed at the source vent, then it was obliterated by subsequent glacier erosion. The lava must have flowed down paleotopography and filled low-laying swales. These paleovalleys are imprinted onto the landscape: where the lava intersects the coastline, it forms elongated headlands that are more resistant to wave attack than the intervening embayments. The lava pinches out against older drift immediately northeast of the exposure, probably marking the edge of a paleovalley. Southwestward, the lava is laterally continuous over several kilometers of coastal bluff. The base of the flow slopes southwestward at $\sim$1 m km^{-1} as the flow thickens from 3 to 5 m. The presence of scoria at the flow top shows that the surface has suffered little posteruption erosion, at least in places. Where exposed, the base is sharp and planar (<10 cm of relief over 10 m lateral exposure) and lacks a brecciated zone or any other evidence for phreatic conditions.

The lava is overlain by 6.8 m of silty gravel with subrounded clasts up to 1 m in diameter, some faceted and striated. The gravel is poorly exposed at the measured section, but in nearby

bluffs is composed of crudely bedded, poorly sorted sand and gravel containing clasts of diverse lithologies. Where they can be traced laterally, beds are commonly deformed by faulting and folding. The gravel makes up the hummocky surface topography around the surrounding landscape, including hillocks and sinuous ridges interpreted as kames and eskers composed of ice-contact stratified drift. The gravel is capped by peat and organic silt that thins over ridges and thickens in swales.

GEOCHRONOLOGY

Radiocarbon

A new AMS ^{14}C age on plant macrofossils from 4.8 m asl yielded an age of >53,600 ^{14}C yr BP (NSRL-10726). This age is consistent with other nonfinite ^{14}C ages obtained from organic matter overlying the early Wisconsin drift elsewhere in the southern Ahklun Mountains (e.g., Kaufman *et al*., 1996). The entire stratigraphic sequence (below the capping peat) is therefore older than the range of ^{14}C dating.

Luminescence Geochronology

Luminescence geochronology is especially effective for dating sediments that have been baked. Three samples of sediment heated by overlying lava were analyzed by thermoluminescence (TL), and the results were reported elsewhere (Kaufman *et al*., 2001). Two of the samples (dated at 59,000 ± 5000 and 78,000 ± 8 yr B.P.) were collected from the exposure described here, and the third sample (dated at 74,000 ± 7000 yr B.P.) was from a coastal exposure (DK96-48) located ~2 km to the southwest (Fig. 2). The average age is 70,000 ± 10,000 yr, which gives the time of the emplacement of the lava.

In this study we also employ a newer variation of the technique—optically stimulated luminescence—to estimate the ages of nearshore marine sediment near the base of the section. TL dating of waterlain sediment can be problematic because of the potential for insufficient solar resetting prior to deposition. Waterlain sediment often receives limited light exposure during deposition because of the light-filtering effects of water and turbidity (Jerlov, 1976). Thus, waterlain sediment may have a residual luminescence level. The recent advent of optical dating, including infrared stimulated luminescence (IRSL) (e.g., Aitken and Xie, 1992), provides a sensitive tool for discriminating inherited from postdepositional luminescence emissions, ultimately providing a better geochronometer for waterlain sediment (e.g., Huntley *et al*., 1985). Previous analysis of modern and ^{14}C-dated Holocene intertidal mud (Kaufman *et al*., 1996) demonstrates that the bulk of sediment in this environment is reset by solar radiation prior to deposition, thereby lending confidence to ages on similar Pleistocene deposits by optical luminescence techniques.

Two samples from the lower lithofacies unit were dated using IRSL. Details of IRSL analytical procedures are given in Table 1 and typical analytical results are shown in Fig. 4. The lower sample, from 2.9 m asl, yielded an age of 151,000 ± 13,000 yr (UIC-687); the upper sample, from 4.1 m asl, was dated at 119,000 ± 10,000 yr B.P. (UIC-688).

TABLE 1
Optically Stimulated Luminescence Data

Lab No. (UIC)	687	688
a count (ks cm^{-2})[a]	0.299 ± 0.015	0.268 ± 0.014
Th (ppm)	2.72 ± 0.43	2.22 ± 0.33
U (ppm)	1.61 ± 0.18	1.51 ± 0.15
Unsealed/sealed[b]	1.02 ± 0.07	0.93 ± 0.07
K_2O (%)[c]	1.65 ± 0.02	1.96 ± 0.02
A value[d]	0.051 ± 0.001	0.045 ± 0.001
Dose rate (Gy (10^3 yr)$^{-1}$)[e]	2.11 ± 0.10	2.23 ± 0.11
Equivalent dose (Gy)[f]	320.51 ± 3.18	264.73 ± 1.58
Age estimate (10^3 yr)	151.2 ± 12.5	118.6 ± 10.2

Note. Optical stimulation was by infrared emissions (880 ± 80 nm) from a ring of 30 diodes (Spooner *et al*., 1990) with an estimated energy delivery of 17 mW cm^{-2}. The output from the diode array at the sample position was calibrated by measuring the current induced in a silicon photodiode (Telefunken BPW-34) connected to a resistive circuit. The resultant blue (Schott BG-39; <5% transmission below 360 nm) emissions from the sediments were monitored. The background count rate for measuring blue emissions was low (80 counts s^{-1}), with a signal to noise ratio of >20. Samples were excited for 90 s, and the resulting IRSL signal was recorded in 1-s increments. The IRSL signal was measured at least 1 day after preheating at 160°C for 5 h (cf Aitken and Xie, 1992). Tests for anomalous fading of the laboratory-induced and preheated IRSL signal, after >32 days of storage, revealed an insignificant (<7%) reduction in signal, indicating stability of the laboratory and natural infrared emissions. Age calculations assume 20 ± 5% moisture content.

[a] Thick-source alpha-count rate; U and Th concentrations calculated from alpha-count rate, assuming secular equilibrium (e.g., Huntley and Wintle, 1981).

[b] Ratio of bulk alpha-count rate under unsealed and sealed counting conditions; a ratio of >0.95 indicates little or no radon loss (Huntley and Wintle, 1981; Jensen and Prescott, 1983).

[c] Percentage of K determined by flame photometry.

[d] Measured alpha efficiency factor (a) as defined by Aitken and Bowman (1975).

[e] Dose rate includes a contribution from cosmic radiation of 0.14 ± 0.01 Gy (10^3 yr)$^{-1}$.

[f] Errors for individual equivalent dose (ED) determinations at a particular light exposure time were determined using a nonlinear least-squares routine, based upon the Levenberg–Marquardt method (Marquardt, 1963), in which inverse variance weighted data are modeled by a saturating-exponential function (Huntley *et al*., 1988). Errors were generated for each ED calculation in a variance–covariance matrix. The resultant uncertainties in ED reflect dispersion in the data and random errors from modeling the data by a saturating exponential function. Standard statistical data weighing procedures were used to calculate an average ED and associated errors.

Tephrostratigraphy

Quaternary tephra beds derived from explosive eruptions of Aleutian Arc and Alaska Peninsula volcanoes are numerous and widespread over southwestern Alaska. Relatively little work has been done in southwestern Alaska on these potentially important stratigraphic markers, although tephra beds have been used elsewhere in Alaska and the Yukon Territory for intra- and inter regional stratigraphic correlations (Westgate *et al*., 1985, 1990; Berger *et al*., 1996; Preece *et al*., 1999). Four tephra beds were

TABLE 2
Average Glass Major-Element Composition of Tephra Beds

Tephra:	Aeolis Mountain				Kulukak Bay			Togiak		Old Crow				
Sample ID:	UT1408		UT1409	UT1435	UT1406		UT1447	UT1411		UT1407	UT1434		UT1577	UT828
Site:	DK95-22		DK96-33	WM97-62	DK95-22		WM97-48	DK96-33		DK95-25	WM97-61		WM98-05	Fairbanks[a]
SiO_2	70.80	(0.20)	70.72 (0.28)	70.70 (0.16)	76.45	(0.20)	76.74 (0.23)	74.97	(0.18)	75.45	(0.25)	75.24	(0.19)	75.10 (0.16)	75.18	(0.21)
TiO_2	0.60	(0.06)	0.58 (0.08)	0.56 (0.09)	0.16	(0.07)	0.16 (0.05)	0.25	(0.06)	0.30	(0.09)	0.31	(0.08)	0.31 (0.03)	0.26	(0.05)
Al_2O_3	14.68	(0.11)	14.65 (0.07)	14.76 (0.10)	13.47	(0.10)	13.32 (0.12)	13.64	(0.11)	13.06	(0.14)	13.15	(0.10)	13.11 (0.10)	13.13	(0.12)
MgO	0.61	(0.03)	0.65 (0.05)	0.61 (0.04)	0.27	(0.03)	0.26 (0.02)	0.21	(0.02)	0.26	(0.02)	0.26	(0.03)	0.27 (0.02)	0.26	(0.01)
FeOt	3.06	(0.11)	3.22 (0.09)	3.06 (0.08)	1.52	(0.06)	1.43 (0.08)	1.72	(0.07)	1.74	(0.04)	1.75	(0.09)	1.70 (0.05)	1.76	(0.06)
MnO	0.10	(0.05)	0.13 (0.04)	0.10 (0.04)	0.11	(0.03)	0.09 (0.04)	0.06	(0.03)	0.07	(0.04)	0.06	(0.04)	0.07 (0.03)	0.06	(0.04)
CaO	2.44	(0.12)	2.45 (0.09)	2.45 (0.07)	1.79	(0.04)	1.75 (0.09)	1.40	(0.08)	1.47	(0.03)	1.49	(0.06)	1.48 (0.06)	1.59	(0.05)
Na_2O	4.60	(0.09)	4.48 (0.16)	4.61 (0.11)	4.19	(0.13)	4.22 (0.08)	4.13	(0.10)	3.75	(0.18)	3.80	(0.14)	3.93 (0.11)	3.82	(0.10)
K_2O	2.96	(0.09)	2.96 (0.07)	2.99 (0.08)	1.91	(0.06)	1.88 (0.08)	3.50	(0.07)	3.63	(0.11)	3.67	(0.09)	3.75 (0.09)	3.66	(0.07)
Cl	0.16	(0.04)	0.16 (0.05)	0.17 (0.03)	0.13	(0.04)	0.14 (0.04)	0.12	(0.03)	0.28	(0.04)	0.27	(0.04)	0.28 (0.03)	0.28	(0.03)
H_2Od	1.40	(1.01)	1.60 (1.59)	1.44 (0.70)	3.81	(0.87)	4.92 (0.91)	3.24	(1.06)	3.55	(1.04)	4.17	(1.24)	5.99 (1.75)	3.53	(0.92)
n	8		9	9	6		15	19		10		20		15	9	

Note. All analyses were done on a Cameca SX-50 wave-length dispersive microprobe operating at 15 kV accelerating voltage, 10- to 15-mm beam diameter, and 6-nA beam current. Standardization was achieved by the use of mineral and glass standards. Analyses were recast to 100% on a water-free basis. ( ), Standard deviation; *n*, number of analyses; FeOt, total iron oxide as FeO; H_2Od, water by difference.

[a] UT828 is from Eva Creek, Fairbanks (see Preece *et al.*, 1999).

FIG. 4. Additive dose build-up curve and residual level for 1 h of filtered sunlight exposure for sample UIC-687 from nearshore marine mud at 2.9 m asl (151,000 ± 13,000 yr B.P.), Togiak Bay site. Infrared stimulated luminescence (IRSL) emissions were measured after 3 s of infrared light exposure. Inset a: shine-down curves for natural and additive dose treatments. Inset b: equivalent dose (De) values for a range of infrared light exposure times.

sampled at the Togiak Bay section. Multiple criteria were used to characterize them, including glass-shard morphology, mineral petrography, and major- and trace-element composition of purified glass-shard separates. Glass major- and trace-element compositions were compared with tephra beds at other sites in southwestern Alaska to check for potential correlations.

All four tephra beds are rhyolitic (Table 2) and are classified as type I, on the basis of their mineral and rare-earth-element (REE) compositions, confirming derivation from volcanoes in the Aleutian Arc and Alaskan Peninsula (Preece *et al.*, 1999). The mineral fraction is dominated by feldspar and Fe–Ti oxides with lesser amounts of orthopyroxene, clinopyroxene, and apatite; amphibole is rarely present and REE have La/Yb <13 (Table 3).

The lowest tephra bed (UT1408, UT1409) marks the base of the third lithofacies unit at 5.1 m asl (Fig. 3). It ranges up to 5 cm thick and, in places, shows two discrete layers of light-tan, silt to medium sand grains separated by up to 1 cm of black silt. The lower layer is thicker and finer grained; the upper layer is coarser and pumice and phenocryst rich. The tephra bed was sampled during consecutive years, UT1408 in 1995 and UT1409 in 1996. Both samples are dominated by low-vesicular pumice and have similar mineralogy and glass major- and trace-element compositions (Tables 2 and 3)—attributes that strongly resemble those of a tephra (UT1435) found in a coastal bluff 25 km to the west at Aeolis Mountain (WM97-62;

TABLE 3
Average Glass Trace-Element Composition of Tephra Beds

Tephra:	Aeolis Mountain		Togiak	Old Crow	
Sample ID:	UT1408a	UT1435a	UT1411b	UT1434b	UT815b
Site:	DK95-22	WM97-62	DK96-33	WM97-61	Fairbanks
Rb	78	62	122	89	92
Sr	—	—	100	113	113
Y	—	—	21	32	34
Zr	—	—	151	223	231
Nb	—	—	4	8	8
Cs	4.18	3.81	8.58	4.19	4.38
Ba	759	666	820	889	959
La	20.42	18.58	15.9	22.14	22.71
Ce	20	46.6	29	43	44
Pr	—	—	3.69	5.62	5.83
Nd	26.3	22.9	13.8	21.8	22
Sm	6.53	6.21	3.02	4.69	4.75
Eu	1.22	1.2	0.75	0.97	0.98
Gd	—	—	2.96	4.74	5
Tb	1.09	0.99	0.49	0.82	0.85
Dy	—	—	2.89	4.81	4.92
Ho	—	—	0.6	0.99	1.05
Er	—	—	1.86	3.01	3.12
Tm	—	—	0.28	0.47	0.52
Yb	4.52	4.65	1.95	3.14	3.23
Lu	0.67	0.68	0.22	0.4	0.38
Hf	6.57	6	4.45	6.4	6.74
Ta	0.56	0.5	0.22	0.51	0.51
Th	7.36	6.74	10.7	9.4	9.1
U	2.87	2.55	6.68	4.61	4.64
Sc	13.36	12.18	—	—	—
n	1	1	3	2	3

Note. Glass shards were separated magnetically and with *s*-tetrabromoethane–acetone mixture. Remaining contaminants were removed by hand under a binocular microscope. All glass separates were washed in 1% HF for 30 s prior to analysis. *n*, Number of analyses. a, Glass separates analyzed by the instrumental neutron activation technique following the methods of Barnes and Gorton (1984). b, Glass separates analyzed by fully quantified solution ICP-MS performed using a VG Elemental ICP-MS PlasmaQuad II+ with a modified high-sensitivity interface and calibration was achieved using multielement synthetic standards. Details of the analytical procedures and standards are given in Pearce *et al.* (1997).

Fig. 2). At this site, the tephra comprises a 50-cm-thick bed at 6.6 to 7.1 m asl. It is enclosed within a 19-m-thick wedge of diamicton containing coarse, angular, locally derived mass-wasted clasts from the adjacent coastal headland. This tephra, herein named Aeolis Mountain tephra, is clearly distinguished from other tephra beds in the region by its relatively low SiO_2 content (Fig. 5).

Another tephra (UT1410) was collected from one of many thin (<0.5 cm) lens and stringers of finer grained, silty interbeds within a sandy unit between 7.0 and 7.2 m asl (Fig. 3). The analyzed sample was from a 0.5-cm-thick lens at 7.1 m asl. Major-element analyses of glass shards revealed that this tephra bed is composed of multiple, dissimilar populations, apparently reworked.

A third tephra (UT1406) is from the base of the uppermost organic-rich silt at 7.5 m asl. The tephra bed is 1 to 5 cm thick and is dominated by bubble-wall shards, stretch pumice, and low-vesicular pumice. The morphology and composition of its glass shards, along with their petrographic features, are similar to another tephra (UT1447) from near Kulukak Bay (Fig. 1). At this site (WM97-48), the 5-mm-thick tephra was found at 11.4 m asl within thin beds of fluvial gravel and colluvial peat above and below ice-contract drift. This tephra, herein named Kulukak Bay tephra, is distinguished from other tephras in the region by its high SiO_2 and low K_2O contents (Fig. 5).

The uppermost tephra bed, herein named Togiak tephra (UT1411), comprises much of a 20-cm-thick zone of convoluted, tan to reddish–brown, organic-rich sandy silt that rests on a deformed base. The purest material was sampled at 7.8 to 7.9 m asl. Reworked tephra is also found above this zone as pods and deformed layers and is disseminated in the organic-rich silt. The glass consists of bubble-wall shards and poorly vesicular shards and pumice. This distinctive, K_2O-rich tephra bed has not been recognized elsewhere in southwestern Alaska (Fig. 5).

The glass-shard morphology, mineralogy, and chemical composition of Togiak tephra are similar to Old Crow tephra (OCt), which occurs at several sites in the area (DK95-25, WM97-61, and WM98-05; Fig. 1), but there are significant compositional differences (Tables 2 and 3). Samples of OCt and Togiak tephra analyzed together under identical instrumental conditions and calibrations show slightly higher Al_2O_3 and slightly lower SiO_2 and Cl contents in Togiak tephra (Fig. 6). Trace-element compositions show even greater differences, with higher Th, U, Cs, and Rb and lower Zr, Nb, and REE in Togiak tephra compared with OCt (Table 3; Fig. 6). If Togiak tephra and OCt were from the same volcano and related to the same magma by closed-system crystal fractionation processes, then trace-element contents should vary systematically. This is not observed, however. For example, because Th and heavy REE (Gd–Lu) are strongly

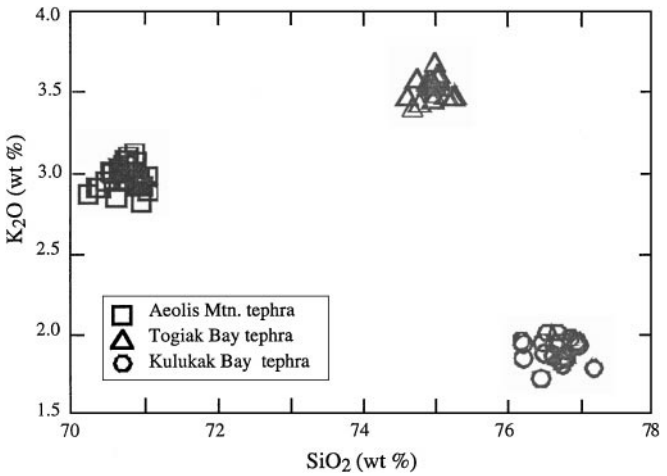

FIG. 5. K_2O versus SiO_2 variation diagram showing the compositional distinctions among individual glass grains from Aeolis Mountain, Togiak, and Kulukak Bay tephras.

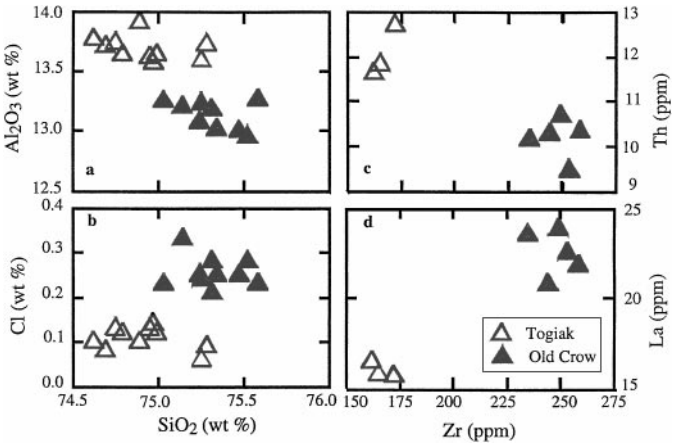

FIG. 6. Major- and trace-element composition of individual glass grains showing differences between Old Crow and Togiak tephras; a and b: Al_2O_3 and Cl versus SiO_2; c and d: La and Th versus Zr.

partitioned into zircon and apatite, these elements should behave similarly if the two tephra beds are related by closed-system processes. Instead, Th behaves antithetically to Zr and the heavy REE (Table 3, Fig. 6). Although it is possible that these two tephra beds are from the same volcano, it would require a complicated petrogenetic history.

Aeolis Mountain, Kulukak Bay, and Togiak tephras have not been found elsewhere in Alaska or the Yukon Territory. Although the tephra beds within the Togiak Bay section do not correlate with previously documented tephra samples, they do provide the essential baseline data for future studies.

PALEOENVIRONMENTAL CHANGES

Diatoms

Fossil diatoms (Bacillariophyceae) were analyzed from 29 samples taken at 20-cm intervals from the stratified sequence below the lava. The primary goals of the diatom investigation were to establish the stratigraphic position of marine regression from the site and to identify lacustrine episodes within the upper portion of the section. Dried sediments (0.2 g) were prepared using standard oxidative techniques (Battarbee, 1986) and examined under oil-immersion light microscopy at 1000×. Freshwater diatom taxonomy follows standard lake floras (Patrick and Reimer, 1966, 1975; Krammer and Lange-Bertalot, 1986–1991; Foged, 1981; Germain, 1981), whereas marine forms were identified in the context of other studies of high-latitude nearshore floras (e.g., Lichti-Federovich, 1983). Diatoms are sparse in many of the freshwater levels and throughout the marine portion of the section; only 8 samples contain countable diatom concentrations. For this reason, diatom abundances have been tabulated on a semi-quantitative four-point abundance scale (Fig. 7). Nonetheless, the diatom flora exhibits dramatic stratigraphic changes, and these relate directly to the succession of depositional environments in the section.

With the exception of two barren samples from 3.6 and 3.8 m asl, sediments from the lower 2 m of the exposure (from 2.6 to 4.6 m asl) contain identifiable fragments of marine diatoms (Fig. 7). The dominance of benthic forms reflects a nearshore paleoenvironment. The transition from a marine to a freshwater depositional environment occurred between 4.6 and 4.8 m asl in the section. Although the sample from 4.8 m asl is dominated by freshwater taxa, this is the only sample in which a brackish taxon (*Diploneis interrupta*) was recorded.

The intervals in the upper section that contain freshwater diatoms (i.e., 4.8 to 8.2 m asl) can further be subdivided into two broadly defined recurrent types. The first are sediments preserving rich diatom floras dominated by small colonial *Fragilaria* spp. and containing planktonic *Aulacoseira* spp. Three such intervals are represented (4.8 to 5.0; 6.4 to 6.6; and 7.8 to 8.0 m asl), and these are inferred to represent a fully lacustrine depositional environment. A perennial lake, likely of sufficient depth to thermally stratify, occupied the site at these times. Alkaliphilous fragilarioid diatoms suggest significant deliveries of catchment-derived base cations, as is frequently observed in late-glacial deposits of temperate lakes (Whitehead *et al*., 1989). Heavily silicified *Aulacoseira* spp. are also associated with the enhanced supply of catchment weathering products, for example, during periods of cooling and associated soil destabilization (Wolfe and Härtling, 1996). Samples intervening between the lacustrine phases in the upper portion of the sequence contain vastly lower diatom valve concentrations that are limited to benthic periphytic genera (*Eunotia, Navicula, Nitzschia,* and *Pinnularia* spp.). Three such intervals are represented: 5.2 to 6.2; 6.8 to 7.6; and 8.2 m asl. The inferred paleoenvironment for these sediments is a shallow and perhaps ephemeral water body lacking the limnological stability to develop diversified benthic and planktonic diatom floras. Many of these diatoms occur commonly in marshes and other waters of high humic content.

Physical Stratigraphy

The physical properties of the sediments, together with the diatom taxa, can be used to interpret the changing depositional environments represented by the lower stratified sequence (Fig. 3). We interpret the ripple and horizontally laminated silty sand of the lowest lithofacies unit as a tidally influenced sand flat or barrier bar. Relative sea level was at least several meters above the present during the deposition of this unit. The transition to massive mud of the second lithofacies unit records the emergence and transformation of the site to a mud-flat or coastal marsh environment as sea level regressed. The diamicton interbedded within the lower, marine section of this lithofacies unit was probably deposited by a mass-wasting process as nearby low hills composed of saturated older drift emerged. Alternatively, the diamicton was shed from the front of a glacier (cf. glacigenic sediment gravity flows of the Nushagak Formation; Lea, 1990). Without definitive evidence for ice proximity, however, we prefer to interpret the bed as colluvium rather than glaciogenic.

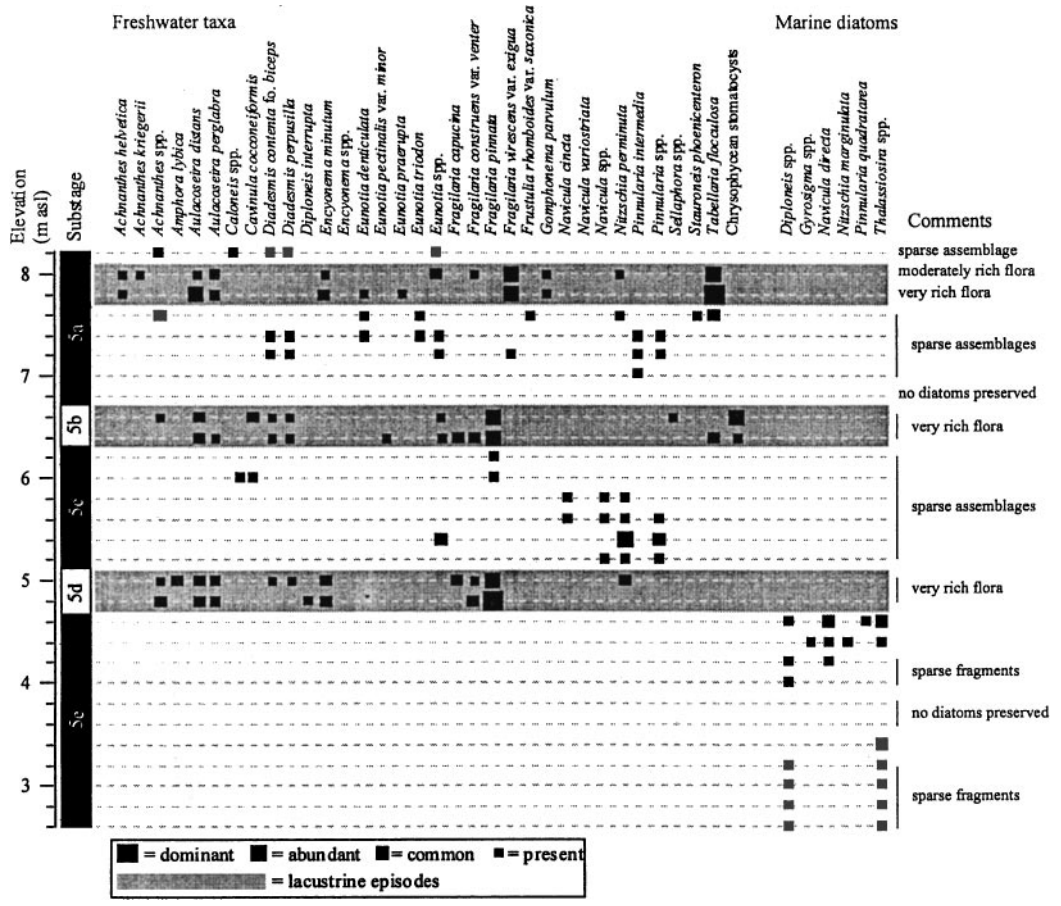

FIG. 7. Diatoms identified in the Togiak Bay section shown in relation to sample elevation and inferred marine oxygen-isotope stages.

Midway through the muddy lithofacies unit, between 4.6 and 4.8 m asl, marine diatoms are replaced by brackish and then by a fresh-water assemblage. We envisage a relatively large lake forming on a freshly emerged, low-lying coastal plain as the sea level lowered. The lake would have occupied a preexisting depression, perhaps originally a tidal channel or lagoon, or a depression within the older drift that underlies the marine sediment. This depression later served as a basin or conduit for the lava flow.

The transition to the sand-dominated upper lithofacies unit at 5.1 m asl might record the input of eolian sand blown off the newly emerged continental shelf or fluvial sand as rivers migrated into the basin. In either case, the lake shallowed, but was not entirely filled by sediment during the interval of shallow water represented between 5.2 and 6.2 m asl. The lake level rose a second time in response to either increased effective precipitation or aggradation of the basin's threshold, and organic-rich silt with lacustrine diatoms was deposited between 6.5 and 6.7 m asl. The lake shallowed once again and littoral or fluvial sand and gravel were deposited over the site. The organic-rich silt that overlies the sand and gravel at 7.5 m asl contains reworked tephra and diatoms indicative of a floodplain environment. The aggradation of floodplain deposits might coincide with a rise in sea level and a consequent reduction in river gradient. A third lake phase is recorded in the diatom assemblage in samples from 7.8 and 8.0 m asl.

By the time the lava erupted, the landscape had emerged fully; the well-exposed base of the flow shows no indication that water was present to interact with the encroaching lava. Sometime after the eruption, an outlet glacier draining the southwestern sector of the Ahklun Mountain ice cap flowed down the Togiak River valley and advanced over the site. The hummocky drift that surrounds Togiak Bay marks either the terminal or a recessional position of this ice.

Pollen

Twenty-nine samples, spaced at 20-cm intervals through the stratified section, were processed according to conventional methods to recover fossil pollen (Faegri *et al.*, 1992). Among them was a surface-sediment sample from an intertidal mudflat near Togiak; the pollen assemblage of this sample should reflect the modern vegetation in the region. Pollen and spore percentages (Fig. 8) were based on the sum of all terrestrial pollen taxa. Three samples (7.0, 7.2, and 8.2 m asl) were barren of pollen, and pollen concentrations were generally low (typically

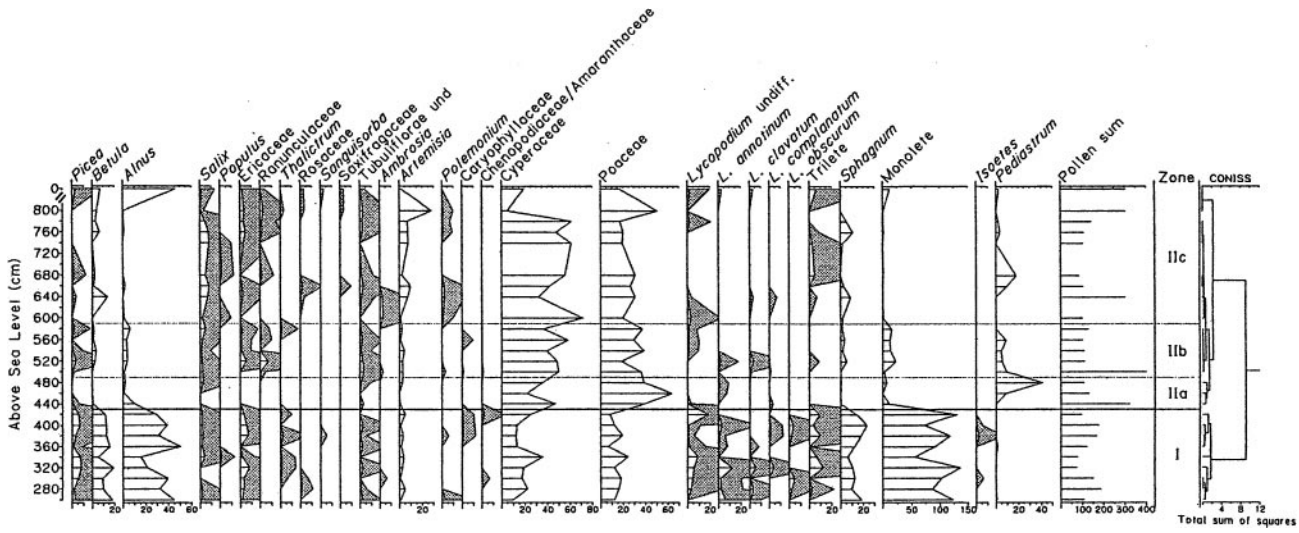

FIG. 8. Pollen percentages from the Togiak Bay section. Stippled curves represent 10× exaggeration. The pollen assemblage at 0 cm above sea level is from a surface-sediment sample from Togiak Bay.

$\ll$10,000 grains g^{-1}) for the remaining samples, which hampered or precluded our goal of counting at least 300 grains per sample.

Despite the low pollen counts, the profile can be divided into two zones based on the characteristics of pollen assemblages (Fig. 8). Below 4.3 m asl, pollen/spore assemblages are dominated by *Alnus* (15–50%), *Betula* (5–19%), and monolete spores (>56%). This zone is also characterized by relatively high percentages of *Picea* pollen (1–8%) and *Sphagnum spores* (6–23%), and low percentages of Cyperaceae (9–36%) and Poaceae (7–24%) pollen. These fossil pollen assemblages are similar to the modern pollen spectra from Togiak Bay (Fig. 8) and other sites in southwestern Alaska (Anderson and Brubaker, 1986; Hu *et al*., 1995), suggesting that the regional vegetation prior to the interval represented by deposits at 4.3 m asl was likely a forest–tundra ecotone similar to that found in the region today. However, the percentages of *Picea* pollen at several levels within this zone are substantially higher than those in the modern surface sample implying that the population density of spruce trees was possibly greater during OIS 5e than today in southwestern Alaska, which might have resulted from warmer climatic conditions.

Above 4.3 m asl, the pollen assemblages are dominated by Cyperaceae (5–61%) and Poaceae (18–65%). *Picea* is absent from most levels, and the percentages of *Betula* and *Alnus* pollen and monolete spores are all much lower than those below 4.3 m asl. A stratigraphically constrained cluster analysis (CONISS in Fig. 8; Grimm, 1987) was used to divide the pollen profile above 4.3 m asl into three subzones. The middle of these three subzones is characterized by a pollen assemblage somewhat similar to those of zone I; *Picea* and *Alnus* pollen and monolete spores increase relative to the other two zones above 4.3 m.

Inferring vegetation and climate from the fossil pollen spectra at this site must be done with caution because of the complex changes in the depositional regime that may affect preservation conditions and source areas of pollen (Faegri *et al*., 1992). Although these variables undoubtedly had an important effect on the pollen record at Togiak Bay, we consider the major shifts in the pollen spectra as reliable indicators of vegetation changes. This reliability is supported by evidence for the relative timing of pollen and sedimentary changes, which are not strictly simultaneous. For example, the pronounced decrease in tree and shrub pollen above 4.3 m asl clearly predates the emergence of the site above sea level and the formation of a lake at 4.8 m asl.

DISCUSSION: CORRELATION WITH MARINE OXYGEN-ISOTOPE RECORD

The IRSL age of 151,000 ± 13,000 yr from the basal marine unit suggests that it is older than the last interglaciation of the Milankovitch-tuned benthic oxygen-isotope record (Imbrie *et al*., 1984). However, the presence of interglacial vegetation and the position of sea level above the present, together with the lack of evidence for either significant glacial–isostatic depression or tectonic uplift, precludes a correlation with OIS 6. The IRSL age overlaps with the age of marine terraces on numerous coasts that have been dated by U-series to ~135,000 yr B.P. (reviewed recently by Zazo, 1999). At ±2 SD, the IRSL age overlaps with the peak of OIS 5e at 125,000 yr B.P., a period when eustatic sea level was ~6 m above the present level (Chappell and Shackleton, 1986). Considering the pollen evidence for warmer-than-present conditions, we correlate the marine unit with the last interglaciation (the Pelukian transgression of Hopkins, 1967) and assign it to OIS 5e.

We further correlate the emergence of the site above sea level (at 4.6 m asl) with the transition from OIS 5e to 5d (Fig. 3). On the basis of the global marine oxygen-isotope record, the age of this transition is 117,000 yr (this and other OIS boundary ages

follow Martinson *et al*., 1987). This age is in agreement with the IRSL age of 119,000 ± 10,000 yr from 0.6 m below the marine-to-terrestrial transition at the Togiak Bay site. We interpret the interval represented by pollen zone 2 as corresponding with OIS 5d (117,000 to 105,000 yr B.P.). The pollen evidence indicates the development of tundra vegetation, and the diatoms indicate a relatively deep, perennial water body, perhaps reflecting lower evaporation rates resulting from decreased temperature and increased lake-ice cover.

We tentatively correlate the reversion to warmer conditions represented by the slight increases in the percentages of *Picea, Betula, Alnus*, and monolete fern in pollen subzone IIb (5.1 to 6.3 m asl) with OIS 5c (105,000 to 93,000 yr B.P.). The diatoms indicate shallow or ephemeral water at the site during this interval, perhaps in response to increased evaporation associated with higher temperatures. Although we lack firm geochronological control, we speculate that the subsequent interval of perennial lacustrine conditions, as evidenced by the diatom and sedimentological data between 6.3 and 6.7 m asl, coincides with OIS 5b (93,000 to 85,000 yr B.P.). The reversion to shallow water suggested by the diatoms indicates that the upper 1.8 m of the stratified sequence records the warmer conditions of OIS 5a (85,000 to 74,000 yr B.P.). No pollen-assemblage change is observed that corresponds to the division of OIS 5b and 5a, however. We suggest that the sand, gravel, and overlying organic-rich silt record floodplain aggradation, which would be expected during OIS 5a when sea level was at most a few meters below the present level (Chappell and Shackleton, 1986). Aggradation would also be expected if the drainage contained an advancing glacier that generated an increased sediment load. Regardless, a correlation with OIS 5a is consistent with the TL age of 70,000 ± 10,000 yr on the overlying lava.

Available geochronology and regional correlations indicate that the drift overlying the lava is early Wisconsin (*s.l.*) in age. The site lies ~30 km downvalley from the limit of a late Wisconsin Ahklun Mountains ice cap (Manley *et al*., 2001) and ~30 km within the limit of the penultimate, more extensive advance of the ice cap (the Arolik Lake glaciation; Briner and Kaufman, 2000). This advance occurred after the last interglaciation (<125,000 yr B.P.), as indicated by the absence of emergent shorelines or beach deposits atop drift and by the presence of a presumed last-interglacial shoreline 2.5 km beyond the drift near Pyrite Point (Fig. 1; Kaufman *et al*., 2001). Similarly, nowhere have we found the OCt atop the drift. Recent ^{36}Cl analyses (Briner, 1998) yielded a surface-exposure age of 53,600 ± 2000 ^{36}Cl yr on boulders at the Arolik Lake glacial limit, ~80 km northwest of the Togiak Bay section (Fig. 1). Finally, the thermoluminescence age estimates for the basalt flow at the Togiak Bay site itself indicate that the drift is younger than 70,000 ± 10,000 yr.

Broader correlations suggest that the maximum early Wisconsin limit of the Ahklun Mountain ice cap was reached time transgressively. Age estimates for related surficial drift near Nushagak Bay, ~100 km east of the Togiak Bay site (Fig. 1), are slightly older. The Nushagak Formation (Lea, 1990) was deposited there at least in part by ice emanating from the Ahklun Mountains, and the Ekuk limit identified by Lea (1990) appears to correlate with the ice limit 30 km south of the Togiak Bay site (Fig. 1; Manley *et al*., 2001). Luminescence and amino acid age estimates converge on an age of 75,000 to 90,000 yr for the Nushagak Formation (Kaufman *et al*., 1996). Evidence for deposition in a tidally influenced marine setting further constrains the age of the Nushagak Formation to a period of relatively high sea level (late during OIS 5; Lea, 1990). In contrast, the drift of the penultimate glaciation in the Togiak Bay area lacks evidence for glacioestuarine deposition, and the available dates suggest that glaciers advanced across the Togiak Bay site after 70,000 yr B.P. (probably during OIS 4). If the Togiak Bay drift is indeed younger than the Nushagak drift, then either the Togiak River valley outlet glacier did not advance as far as Togiak Bay during OIS 5 or we failed to recognize evidence for ice cover. Regardless of whether the drift of Togiak Bay correlates with the Nushagak Formation to the east, we can confidently assign it to a pre-late-Wisconsin advance of the late Pleistocene.

CONCLUSION

The physical stratigraphy and the paleoecological indicators at the Togiak Bay site record environmental changes during the last interglacial to glacial transition. The 50,000-yr transition was not an interval of steady cooling following the peak of the last interglaciation, but was marked by an interval when trees and shrubs returned to the site, which we tentively correlate with OIS 5c, and by two intervals when a relatively deep lake formed, possibly during OIS 5d and 5b.

The most dramatic change in sedimentology was driven by fluctuations in global sea level, which, in turn, were modulated by the mass balance of distant ice sheets. The position of the shoreline not only controlled the depositional setting, but also directly affected the ecology of the site by modulating its continentality. The extent to which the environmental changes were strictly the result of fluctuating eustatic sea level versus the result of paleoclimatic change driven by other boundary conditions is not known. The relative influence of shoreline geography versus other features of the climate system can be addressed as sites like Togiak Bay are linked with others from the interior of Alaska and from offshore. Tephras, such as those documented here, provide the stratigraphic markers needed for precise chronological control. Regional paleoclimate models will be needed to provide the climatological context for these changes.

ACKNOWLEDGMENTS

We thank A. Krumhardt, M. Edwards, B. Hansen, B. Lee, and R. Teed for pollen analysis; G. Malia for MS, TOC, and grain size analyses; P. Hamilton and J. Smol for initial diatom analyses; N. Pearce and W. Perkins for guidance on ICP-MS analyses; C. Cermigniani and M. Gorton for help with microprobe and neutron activation analyses; T. Hamilton and C. Schweger for their helpful

comments. The Dillingham office of the Togiak National Wildlife Refuge provided critical logistical support; Twin Hills Native Corporation allowed access to their land. This research was supported by the National Science Foundation, Arctic Natural Sciences (OPP-9529940), with additional funding to Preece and Westgate from the Natural Sciences and Engineering Research Council of Canada. This is PARCS contribution No. 158.

REFERENCES

Aitken, M. J., and Bowman, S. G. E. (1975). Thermoluminescent dating: Assessment of alpha particle contribution. *Archaeometry* **17,** 132–138.

Aitken, M. J., and Xie, J. (1992). Optical dating using infrared diodes: Young samples. *Quaternary Science Reviews* **11,** 147–152.

Anderson, P. M., and Brubaker, L. B. (1986). Modern pollen assemblages from northern Alaska. *Review of Palaeobotany and Palynology* **46,** 273–291.

Barnes, S. J., and Gorton, M. P. (1984). Trace element analysis by neutron activation with a low flux reactor (Slowpoke–II): Results for international reference rocks. *Geostandards Newsletter* **8,** 17–23.

Battarbee, R. W. (1986). Diatom analysis. In "Handbook of Holocene Palaeoecology and Palaeohydrology" (B. E. Berglund, Ed.), pp. 527–570. Wiley, Chichester.

Berger, G. W., Péwé, T. L., Westgate, J. A., and Preece, S. J. (1996). Age of Sheep Creek tephra (Pleistocene) in central Alaska from thermoluminescence dating of bracketing loess. *Quaternary Research* **45,** 263–270.

Brigham-Grette, J., and Hopkins, D. M. (1995). Emergent marine record and paleoclimate of the last interglaciation along the northwest Alaskan coast. *Quaternary Research* **43,** 159–173.

Brigham-Grette, J., Hopkins, D. M., Benson, S. L., Heiser, P., Ivanov, V. F., Basilyan, A., and Pushkar, V. (2001). Last interglacial sea level record and Stage 5 glaciation of Chukotka Peninsula and St. Lawrence Island. *Quaternary Science Reviews* **20,** 419–436.

Briner, J. P. (1998). "Late Pleistocene Glacial Chronology of the Western Ahklun Mountains, Southwestern Alaska." Unpublished Mater's Thesis, Utah State University.

Briner, J. P., and Kaufman, D. S. (2000). Late Pleistocene glacial history of the southwestern Ahklun Mountains, Alaska. *Quaternary Research* **53,** 13–22.

Carter, L. D., Hamilton, T. D., and Galloway, J. P. (1989). Late Cenozoic history of the interior basins of Alaska and the Yukon. *U.S. Geological Survey Circular 1026*, 114 p.

Chappell, J., and Shackleton, N. J. (1986). Oxygen isotopes and sea level. *Nature* **324,** 137–140.

Eyles, N., and Miall, A. D. (1984). Glacial facies, In "Facies Models" (R. G. Walker, Ed.), pp. 15–38. Geoscience Canada, Geological Association of Canada.

Faegri, K., Kaland, P. E., and Kryzywinski, K. (1992). "Textbook of Pollen Analysis." Hafner, New York.

Foged, N. (1981). "Diatoms in Alaska." J. Cramer Verlag, Vaduz (Lichenstein).

Gallant, A. L., Binnian, E. F., Omernik, J. M., and Shasby, M. B. (1995). Ecoregions of Alaska. *U.S. Geological Survey Professional Paper 1567*.

Germain, H. (1981). Flore des diatomées, eaux douces et saumâtres du Massif Armoricain et des contrées voisines d'Europe occidentale. Paris: Société Nouvelle des Éditions Boubée.

Grimm, E. (1987). CONISS: A Fortran 77 program for stratigraphically constrained cluster analysis by the method of incremental sum of squares. *Computers and Geosciences* **13**, 13–35.

Hamilton, T. D., and Brigham-Grette, J. (1991). The last interglaciation in Alaska: Stratigraphy and paleoecology of potential sites: *Quaternary International* **10–12,** 49–71.

Hoare, J. M., and Coonrad, W. L. (1961a). Geologic map of the Goodnews Quadrangle, Alaska. *U.S. Geological Survey Miscellaneous Geologic Investigations Map I-339.*

Hoare, J. M., and Coonrad, W. L. (1961b). Geologic map of the Hagemeister Island Quadrangle, Alaska. *U.S. Geological Survey Miscellaneous Geologic Investigations Map I-321*.

Hoare, J. M., and Coonrad, W. L. (1978a). Geologic map of the Goodnews and Hagemeister Island quadrangles region, southwestern Alaska. *U.S. Geological Survey Open File Report 78-9-B.*

Hoare, J. M., and Coonrad, W. L. (1978b). A tuya in Togiak Valley, southwest Alaska. *Journal of Research of the U.S. Geological Survey* **6,** 193–201.

Hopkins, D. M. (1967). Quaternary marine transgressions in Alaska, In "The Bering Land Bridge" (D. M. Hopkins, Ed.), pp. 47–90. Stanford University Press, Stanford, CA.

Hu, F. S., Brubaker, L. B., and Anderson, P. M. (1995). Postglacial vegetation and climate change in the northern Bristol Bay region, southwestern Alaska. *Quaternary Research* **43,** 382–392.

Huntley, D. J., and Wintle, A. G. (1981). The use of alpha scintillation counting for measuring Th-230 and Pa-231 contents of ocean sediments. *Canadian Journal of Earth Sciences* **18,** 419–432.

Huntley, D. W., Godfrey-Smith, D. I., and Thewalt, M. L. W. (1985). Optical dating of sediments. *Nature* **313,** 105–107.

Huntley, D. J., Berger, G. W., and Bowman, S. G. E. (1988). Thermoluminescence responses to alpha and beta irradiations, and age determinations when the high dose response is non-linear. *Nuclear Tracks and Radiation Measurements* **105,** 279–284.

Imbrie, J., and eight others (1984). The orbital theory of Pleistocene climate—Support from a revised chronology of the marine δ^{18}O record. In "Milankovitch and Climate, Part 1" (A. Berger, *et al*. Ed.), pp. 269–305. Reidel, Massachusetts.

Jensen, H. E., and Prescott J. R. (1983). The thick-source alpha particle counting technique: Comparisons with other techniques and solutions to the problem of overcounting. *PACT* **9,** 25–35.

Jerlov, N. G. (1976). "Marine Optics," p. 231. Elsevier, New York.

Kaufman, D. S., Forman, S. L., Lea, P. D., and Wobus, C. W. (1996). Age of pre-late-Wisconsin glacial-estuarine sedimentation, Bristol Bay, Alaska. *Quaternary Research* **45,** 59–72.

Kaufman, D. S., Manley, W. F., Forman, S., and Layer, P. (2001). Pre-late-Wisconsin glacial history, coastal Ahklun Mountains, southwestern Alaska—New amino acid, thermoluminescence, and ^{40}Ar/^{39}Ar results. *Quaternary Science Reviews* **20,** 337–352.

Krammer, K., and Lange-Bertalot, H. (1986–1991) Bacillariophyceae 1 Teil: Naviculaceae (1986); 2 Teil: Bacillariaceae, Epithemiaceae, Surirellaceae (1988); 3 Teil: Centrales, Fragilariaceae, Eunotiaceae (1991a); 4 Teil: Achnanthaceae, Kritische Ergänzungen zu Navicula (Lineolatae) und Gomphonema Gesamtliteraturverzeichnis (1991b). In "Sübwasserflora von Mitteleuropa 2/1-4" (H. Ettl, H. Gerloff, H. Heynig, and D. Mollenhauer, Eds.), Gustav Fischer Verlag, Stuttgart.

Lea, P. D. (1990). Pleistocene glacial tectonism and sedimentation on a macrotidal piedmont coast, Ekuk Bluffs, southwestern Alaska. *Geological Society of America Bulletin* **102,** 1230–1245.

Lichti-Federovich, S. (1983). A Pleistocene diatom assemblage from Ellesmere Island, Northwest Territories. Geological Survey of Canada Paper 83–9, Ottawa.

Manley, W. F., Kaufman, D. S., and Briner, J. P. (2001). Late Quaternary glacial history of the southern Ahklun Mountains, southeast Beringia—Soil development, morphometric, and radiocarbon constraints. *Quaternary Science Reviews* **20,** 353–370.

Marquardt, D. W. (1963). An algorithm for least-squares estimation of non-linear parameters. *Journal of the Society of Industrial and Applied Mathematics* **11,** 431–441.

Martinson, D. G., Pisias, N. G., Hays, J. D., Imbrie, J., Moore, T. C., and Shackleton, N. J. (1987). Age dating and the orbital theory of the Ice Ages: Development of a high-resolution 0 to 300,000 yr chronostratigraphy. *Quaternary Research* **27,** 1–29.

Matthews, J. V., Jr. (1991). Last interglacial in Arctic and subarctic: *EOS* (*American Geophysical Union Transactions*), July 9, 1991, p. 299.

Patrick, R., and Reimer, C. W. (1966). The Diatoms of the United States exclusive of Alaska and Hawaii. Academy of Natural Sciences of Philadelphia Monograph 13 Volume 1.

Patrick, R., and Reimer, C. W. (1975). The Diatoms of the United States exclusive of Alaska and Hawaii. Academy of Natural Sciences of Philadelphia Monograph 13 Volume 2 Part 1.

Pearce, J. G., Perkins, W. T., Westgate, J. A., Gorton, M. P., Jackson, S. E., Neal, C R., and Chenery, S. P. (1997). A compilation of new and published major and trace element data for NIST SRM 610 and NIST SRM 612 glass reference materials. *Geostandards Newsletter* **21,** 115–144.

Péwé, T. L., Berger, G. W., Westgate, J. A., Brown, P. M., and Leavitt, S. W. (1997). Eva interglaciation forest bed, unglaciated east-central Alaska: Global warming 125,000 years ago. *Geological Society of America Special Paper 319*.

Preece, S. J., Westgate, J. A., Stemper, B. A., and Péwé, T. L. (1999). Tephrochronology of late Cenozoic loess at Fairbanks, central Alaska. *Geological Society of America Bulletin* **111,** 71–90.

Schweger, C. E., and Matthews, J. V., Jr. (1991). The last (Koy-Yukon) interglaciation in the Yukon: Comparisons with Holocene and interstadial pollen records. *Quaternary International* **10–12,** 85–94.

Spooner, N. A., Aitken, M. J., Smith, B. W., Franks, M., and McElroy, C. (1990). Archaeological dating by infrared-stimulated luminescence using a diode array. *Radiation Protection Dosimetry* **34,** 83–86.

Westgate, J. A., Stemper, B. A., and Péwé, T. L. (1990). A 3 m.y. record of Pliocene–Pleistocene loess in interior Alaska. *Geology* **18,** 858–861.

Westgate, J. A., Walter, R. C., Pearce, G. W., and Gorton, M P. (1985). Distribution, stratigraphy, petrochemistry, and paleomagnetism of the late Pleistocene Old Crow tephra in Alaska and the Yukon. *Canadian Journal of Earth Sciences* **22,** 893–906.

Whitehead, D. R., Charles, D. F., Jackson, S. T., Smol, J. P., and Engstrom, D. R. (1989). The developmental history of Adirondack (N.Y.) lakes. *Journal of Paleolimnology* **2,** 185–206.

Wolfe, A. P., and Härtling, J. W. (1996). The late Quaternary development of three ancient tarns on southwestern Cumberland Peninsula, Baffin Island, Arctic Canada: Paleolimnological evidence from diatoms and sediment chemistry. *Journal of Paleolimnology* **15,** 1–18.

Zazo, C. (1999). Interglacial sea levels. *Quaternary International* **55,** 101–119.